IOSR Journal of Mechanical and Civil Engineering (IOSR-JMCE)
e-ISSN: 2278-1684,p-ISSN: 2320-334X, Volume 15, Issue 2 Ver. V (Mar. - Apr. 2018), PP 46-65
www.iosrjournals.org

Performance Study of Once-Through Solar Water Heater

Rajendra Karwa[1,*], Chandresh Sharma[2,b]
[1]*Jodhpur Institute of Engineering & Technology*
N. H. 65, New Pali Road, Mogra
Jodhpur (Rajasthan), India 342802
[2]*Jodhpur National University, Narnadi, Jhanwar Road*
Jodhpur (Rajasthan), India
[*]*Corresponding author: Rajendra Karwa*

Abstract: *The paper presents a detailed mathematical model for performance study of a once-through solar water heater. The model is validated against experimental results. It has been utilized to study the solar water heater performance for a range of design, ambient and operating parameters, and heat transfer enhancement on thermal efficiency and pressure drop. The collector with selective coating (ε = 0.1) has a thermal performance advantage of 9-16% depending on the flow rate. A collector with 2 mm thick fins brazed or 0.5 mm thick fins laser or ultrasonic welded have practically the same performance. Use of the heat transfer enhancement devices, such as a twisted tape, can improve the thermal efficiency of the collector by 5.3-6.2% for three times heat transfer enhancement. The results of the study are presented in the form of design plots along with the results of variations in various parameters.*

Keywords: *Once-through solar water heater (collector), mathematical model, heat transfer enhancement, performance study, design plots*

Date of Submission: 18-04-2018 Date of acceptance: 05-05-2018

I. Introduction

A flat-plate collector is heart of a common solar water heater system. There are two types of solar water heater systems: passive and active (forced circulation) type. The passive systems depend on natural convection (thermosyphon effect) to circulate water through the collector tubes. The active or forced circulation systems consist of a pump to circulate water in the system. They are employed in industrial applications. An alternative of the forced system is the once-through system proposed by Wang et al. [1], which is depicted in Fig. 1. In this system, the cold water enters the collector tubes from the lower end and the hot water flows out of the upper end of the tubes without any re-circulation in the system. The driving force for the flow through the collector tubes is the head of the cold water supply, which is usually the tap water. Hot water may be collected in a tank, which can be placed at a convenient place below the collector even inside the building. Thus the load on the roof is cut down significantly.

The most commonly used design of the flat-plate collector, termed as a tube-in-fin design, employs a number of parallel copper tubes equally spaced and bonded with copper plates, which work as fins. The sun facing side of the tubes and plate assembly, termed as absorber surface or simply absorber, is painted black to impart high absorptance for the solar radiation. Generally one or two glass covers are placed at a gap on the top of the absorber surface to arrest heat loss from the top of the absorber to the ambient. The collector assembly is installed at a suitable angle to the horizontal facing south in northern hemisphere. The solar radiation incident on the collector plane passes through the transparent covers and is absorbed at the blackened absorber surface. A part of this absorbed radiation is transferred to the water flowing through the tubes while the remaining part is lost to the ambient by radiation and convection heat transfer because the absorber surface is at a higher temperature than the ambient temperature. It is to note that the thermal performance of a solar water heater is a function of its design and ambient parameters, and water flow rate.

The efforts of the researchers have been directed towards enhancing the thermal performance of solar water heater by various techniques such as use of selective coating on the absorber surface, increased number of glass covers over the absorber, optimization of tube diameter and spacing, etc. These techniques have been successfully used in the past [2]. In the once-through system with fin-in-tube design, the water flows through the collector tubes at very low Reynolds number (in the laminar regime) resulting in a low value of the heat transfer coefficient**.** Thus one of the strategies for the thermal efficiency improvement can be the heat transfer enhancement from the collector tubes to the flowing water. The heat transfer enhancement, while transferring greater amount of heat to the water, reduces the temperature of the absorber surface and thus the heat loss from the collector is also reduced. Since at low flow rates the collector operates with a higher temperature of the

absorber surface leading to a greater heat loss, this strategy is more effective at these flow rate conditions. Extended surfaces, inserts, swirl flow devices, etc have been used as heat transfer enhancement devices. Swirl-flow devices have been used for more than a century to improve heat transfer in industrial heat exchangers. These devices include inlet vortex generators, twisted-tape inserts, etc. Twisted tapes have been suggested for heat transfer enhancement in case of laminar flow [3, 4].

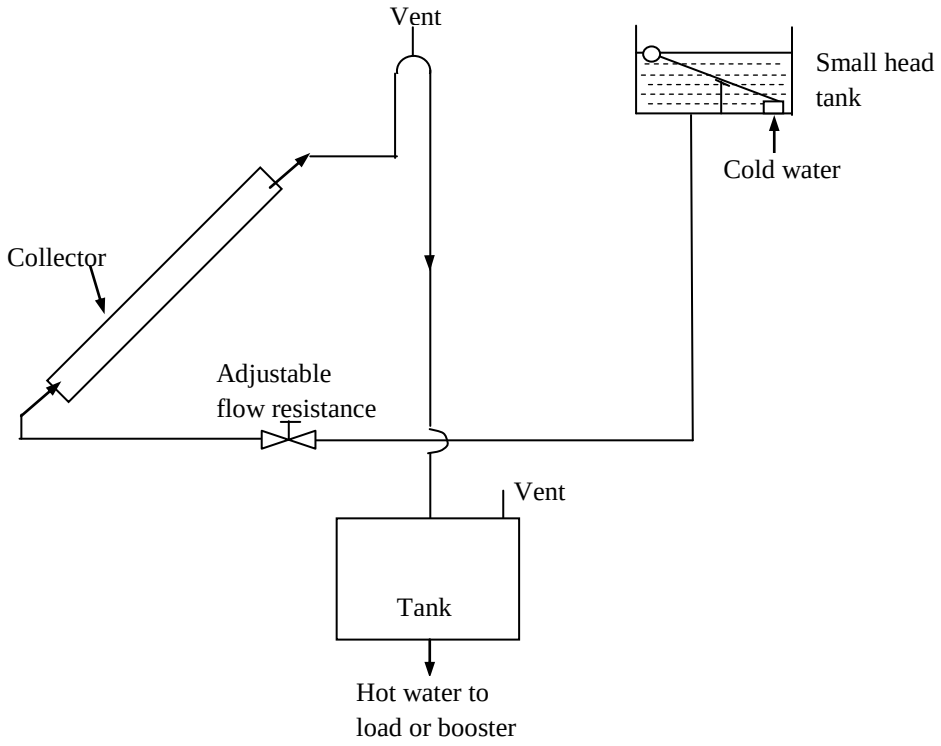

Fig. 1 Schematic diagram of a self-adjusting once-through solar water heater system.

Various twisted tape forms, arrangements and combinations have been identified by researchers for heat transfer enhancement [5-15]. A typical twisted tape is shown in Fig. 2. Heat transfer enhancement (Nu_R/Nu_s, the ratio of Nusselt number Nu_R for the tube with twisted tape to the Nusselt number Nu_s for the smooth tube) is reported to be of the order of 1.5-9.5 depending on the flow Reynolds number and type of enhancement device. In general, the heat transfer enhancement increases with the decreasing twist ratio *y* (ratio of twist pitch *H* to tape width *w*) of the twisted tape and increasing Reynolds number. The accompanying friction factor enhancement is of the order of 1.9 - 27. Heat transfer coefficients and friction factors in a tube fitted with the broken twisted tape are reported to augment by 1.28–2.4 and 2–4.7 times, respectively, of those in the tube fitted with the smooth twisted tape [7]. Thermo-hydraulically, when both heat transfer and friction factor enhancements are considered together, the twisted tape inserted tubes provide better performance than smooth tubes [5- 7, 16[. It can be inferred from these studies that twisted tapes can be employed for performance enhancement of the solar water heater with low Reynolds number laminar flow such as once-through solar water heater. Since the heat transfer enhancement is accompanied with significant increase in friction factor, the choice of the enhancement device depends on the thermohydraulic consideration.

Literature survey shows that the domestic solar water heater has been thoroughly investigated [2, 6, 11-13] but despite its application in industries, the once-through solar water has not been extensively studied since it was proposed by Wang et al. in 1982. Effect of variation of design and ambient parameters, and flow rate over a range, and the effect of the use of the heat transfer enhancement devices on the performance of the once-through solar water heater can be studied by using a mathematical model. However, literature survey shows that such mathematical model is not available. Hence, the objective of the present work is to develop a mathematical model of the once-through solar water heater, which can be utilized by a designer for the development of the smooth tube and enhanced performance solar water heaters. The model is to be utilized for the study of the effect of design and ambient parameters, and water flow rate on the performance of the once-through solar water heater.

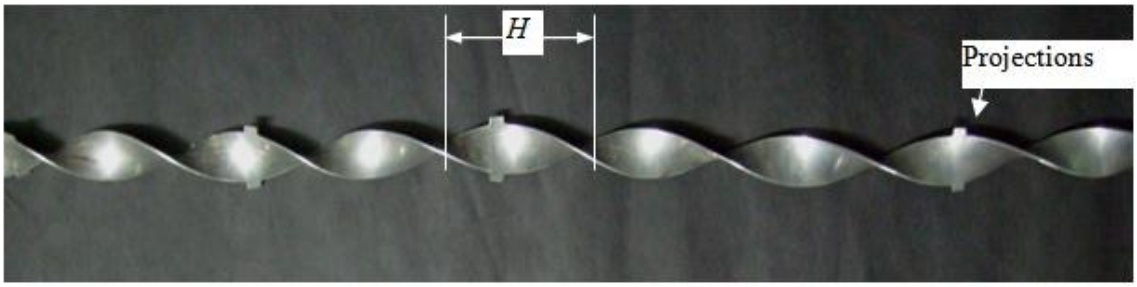

Fig. 2 A 75% width twisted tape (Sharma and Karwa, 2014).

II. Mathematical Model

A mathematical model for the performance prediction of the once-through solar water heater is presented here. The model calculates the useful heat gain by matching the fin base temperature from the iterative solution of basic heat transfer equations of top loss and the tube wall temperature from the consideration of convective heat transfer to the water.

Heat transfer from the heated absorber surface (the surface of the fin and tube exposed to solar radiation) at a mean temperature T_{pm} to the inner surface of the glass cover at temperature T_{gi} takes place by radiation and convection, refer Fig. 3. Hence,

$$q_{tpg} = A_c \left[\frac{\sigma({T_{pm}}^4 - {T_{gi}}^4)}{\frac{1}{\varepsilon_p} + \frac{1}{\varepsilon_g} - 1} + h_{pg}(T_{pm} - T_{gi}) \right], \quad (1)$$

where ε_p and ε_g are emissivities of the absorber surface and glass cover, respectively, and h_{pg} is convective heat transfer coefficient between the absorber and glass cover constituting a parallel plate configuration. A_c is area of the collector.

Heat flows by conduction from the inner surface of the glass cover at temperature T_{gi} to the outer surface at temperature T_{go}. Hence,

$$q_{tg} = k_g A_c \frac{(T_{gi} - T_{go})}{\delta_g}, \quad (2)$$

where k_g is the thermal conductivity of the glass and δ_g is thickness of glass cover.

From the outer surface of the glass cover, the heat is rejected by radiation to the sky at temperature T_s and by convection to the wind blowing over the cover at ambient temperature T_a. Hence,

$$q_{tgo} = A_c \left[\sigma \varepsilon_g ({T_{go}}^4 - {T_s}^4) + h_w (T_{go} - T_a) \right], \quad (3)$$

where h_w is wind heat transfer coefficient, which is a function of the wind velocity.

When thermal equilibrium is established,

$$q_{tpg} = q_{tg} = q_{tgo} = q_t, \quad (4)$$

where q_t is the top loss.

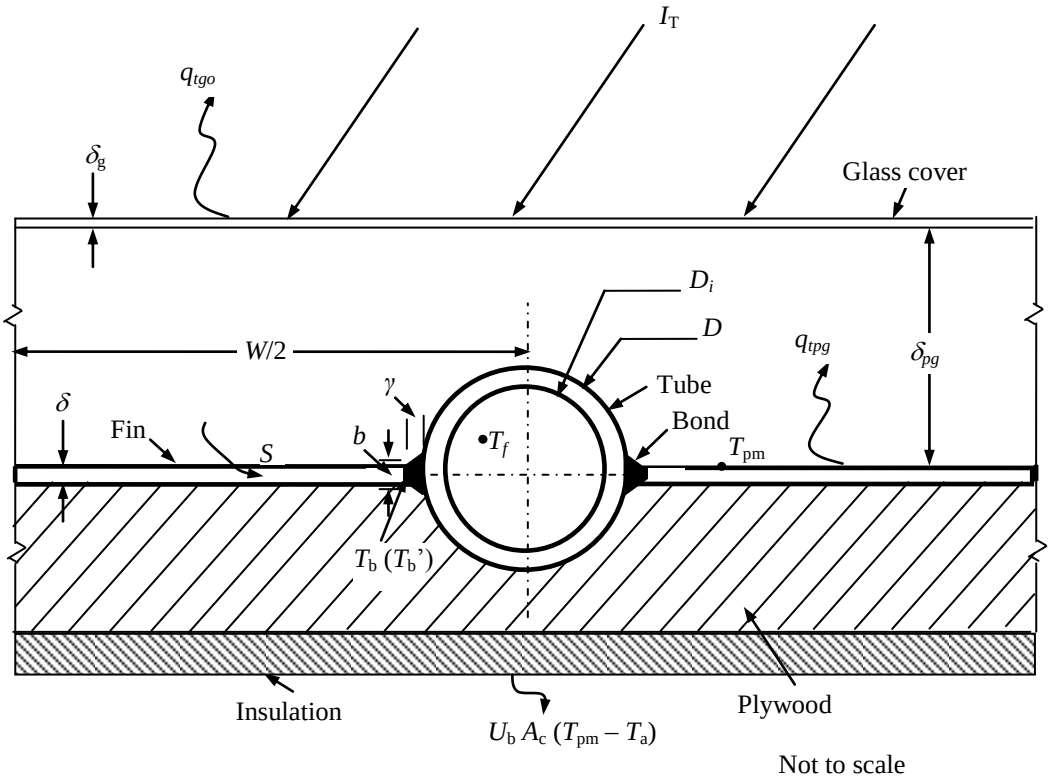

Fig. 3 Cross-section of the solar water heater and heat flow.

The wind heat transfer coefficient has been estimated from McAdams [17] correlation:

$$h_w = 5.6214 + 3.912 V_w \quad \text{for } V_w \le 4.88 \text{ m/s} \tag{5}$$

where V_w is the wind velocity in ms^{-1}.

For the estimate of sky temperature, widely used relation due to Swinbank [18] for clear sky has been used in the present model. The relation is

$$T_s = 0.0552 T_a^{1.5}, \tag{6}$$

where T_s and T_a are expressed in degree Kelvin.

For the estimate of the heat transfer coefficient h_{pg} between the absorber surface and glass cover, the following three-region correlation of Buchberg et al. [19] has been used.

$$\text{Nu} = 1 + 1.446 \times \left(1 - \frac{1708}{\text{Ra}'}\right)^{+} \tag{7a}$$

for $1708 \le \text{Ra}' \le 5900$

(the + bracket goes to zero when negative)

$$\text{Nu} = 0.229 (\text{Ra}')^{0.252} \tag{7b}$$

for $5900 < \text{Ra}' \le 9.23 \times 10^4$

$$\text{Nu} = 0.157 (\text{Ra}')^{0.285}, \tag{7c}$$

for $9.23 \times 10^4 < \text{Ra}' \le 10^6$,

where Ra′ (= Ra cosβ) is the Rayleigh number for the inclined air layers in the gap between the absorber and glass cover. β is the slope or tilt of the collector with the horizontal. The Rayleigh number Ra for the parallel plates is given by

$$\mathrm{Ra} = \left[\frac{g(T_{pm} - T_{gi})\delta_{pg}^{\ 3}}{T_{mpg}\nu_{mpg}^{\ 2}} \right] \mathrm{Pr}_{air}, \tag{8}$$

where δ_{pg} is the gap between the absorber surface and glass cover, and ν_{mpg} is kinematic viscosity of the air at temperature T_{mpg}, which is mean of temperatures of absorber and glass cover. Pr_{air} is the Prandtl number of air at temperature T_{mpg}.

From the calculated value of the top loss, the top loss coefficient is determined from:

$$U_T = \frac{q_t}{A_c(T_{pm} - T_a)}. \tag{9}$$

The collector back loss coefficient is calculated from:

$$U_b = \left(\frac{\delta_{ply}}{k_{ply}} + \frac{\delta_i}{k_i} + \frac{1}{h_b} \right)^{-1}, \tag{10}$$

where δ_{ply} and δ_i are plywood and insulation thicknesses of thermal conductivity k_{ply} and k_i, respectively. h_b is the heat transfer coefficient on the back surface of the collector. Klein [20] specifies h_b = 12.5-25 $\mathrm{Wm^{-2}K^{-1}}$.

The edge loss coefficient has been estimated from [2]:

$$U_e = \frac{U_b A_e}{A_c}, \tag{11}$$

where A_e is area of edge of the collector.

The total loss coefficient U_L is

$$U_L = U_T + U_b + U_e. \tag{12}$$

Knowing U_L, the useful heat gain,

$$q_u = A_c[S - U_L(T_{pm} - T_a)], \tag{13}$$

where S is the solar radiation absorbed by the absorber surface, which equals $I_T(\tau\alpha)_{av}$. I_T is the sum of the beam, diffuse and ground reflected solar radiation on the collector plane, τ is the transmissivity of the glass cover and α is the absorptivity of the absorber surface. $(\tau\alpha)_{av} = 0.96(\tau\alpha)_{beam}$ when beam fraction is high [2]. For small angle of incidence of the solar radiation on the collector plane, $(\tau\alpha)_{beam} \approx \tau \times \alpha$.

The fin base temperature T_b, refer Fig. 3, is [2]

$$T_b = \frac{1}{U_L}\left\{ S - \frac{q_u}{L[(W-D)F + D]} \right\} + T_a, \tag{14}$$

where F is fin efficiency, W is the width of the fin per tube, L is the length of the collector and D is the outer diameter of the tube. The fin efficiency is given by Duffie and Beckman [2] as

$$F = \frac{\tanh[m'(W-D)/2]}{[m'(W-D)/2]}, \tag{15}$$

where m' is fin parameter. For fin of thickness δ and thermal conductivity k, it is defined as [2]

$$m' = \left(\frac{U_L}{k\delta} \right)^{1/2}. \tag{16}$$

From the first law, the mean water temperature

$$T_{fm} = T_i + \frac{1}{2}\left(\frac{q_u}{mc_p}\right), \tag{17}$$

where T_i is the inlet temperature of water, m is the mass flow rate of the water through the collector tube and c_p is specific heat of water.

The mass velocity of water through the tube of inside diameter D_i,

$$G_m = \frac{m}{(\pi/4)D_i^{\,2}}. \tag{18}$$

Flow Reynolds number,

$$\mathrm{Re} = \frac{G_m D_i}{\mu_f}, \tag{19}$$

where μ_f is the dynamic viscosity of the water at its mean temperature.

The thermal entrance length L_{th} for thermally developing flow under the uniform wall heat flux condition is [21]

$$\frac{L_{th}}{D_i} = 0.043\ \mathrm{Re}\ \mathrm{Pr}, \tag{20}$$

where Pr is the Prandtl number of water at its mean temperature.

Nusselt number equation for the fully developed forced laminar flow in a circular tube under the uniform wall heat flux condition is

$$\mathrm{Nu}_{forced} = 4.364. \tag{21a}$$

For thermally developing flow [21],

$$\mathrm{Nu}_{forced} = 4.364 + 0.0722\,\mathrm{Re}\,\mathrm{Pr}\left(\frac{D_i}{L}\right). \tag{21b}$$

From the known value of the Nusselt number, the heat transfer coefficient is calculated from:

$$h_{fi} = \frac{\mathrm{Nu}_{forced} k_f}{D_i}, \tag{22}$$

where k_f is the thermal conductivity of water at its mean temperature.

The resistances to heat flow to the water results from the bond and the tube-to-fluid resistance [2], which gives the fin base temperature as

$$T_b' = T_{fm} + \frac{q_u}{L}\left(\frac{1}{h_{fi}\pi D_i} + \frac{1}{C_b}\right), \tag{23}$$

where C_b (= $k_b b/\gamma$) is bond conductance. k_b is thermal conductivity of bond material, b is bond width and γ is bond thickness.

The thermophysical properties of the water have been taken at the mean temperature of water from the following relations obtained by correlating the data from Holman [22].

$$c_p = 0.027t^2 - 2.0316t + 4211.8 \tag{24a}$$

$$\mathrm{Pr} = 0.0031t^2 - 0.3237t + 12.255 \tag{24b}$$

$$\mu_f = (0.3683t^2 - 40.042t + 1665.2) \times 10^{-6} \tag{24c}$$

$$k_f = 0.0016\,t + 0.5693 \tag{24d}$$

$$\rho_f = -0.0043t^2 - 0.0255t + 999.9, \tag{24e}$$

where $t = T_{fm}$ - 273 (in ^oC).

Temperature rise of the water through the collector tube is

$$\Delta T = \frac{q_u}{mc_p}. \tag{25}$$

The outlet temperature of the water is

$$T_o = T_i + \Delta T. \tag{26}$$

The thermal efficiency of the collector is given by

$$\eta = \frac{q_u}{I_T A_c}. \tag{27}$$

The collector efficiency factor is given by [2]

$$F' = \frac{1/U_L}{W\left\{\frac{1}{U_L[D + (W - D)F]} + \frac{1}{C_b} + \frac{1}{\pi D_i h_{fi}}\right\}}. \tag{28}$$

The useful heat gain from known value of *F'* is

$$q_u{}' = A_c F'\left[S - U_L(T_{fm} - T_a)\right] \tag{29}$$

The outlet water temperature is also given by [2]:

$$T_o{}' = \left[T_i - T_a - \frac{I_T(\tau\alpha)}{U_L}\right]\exp\left(-\frac{A_c U_L F'}{mc_p}\right) + \left[T_a + \frac{I_T(\tau\alpha)}{U_L}\right]. \tag{30}$$

A heat removal factor is defined as

$$F_R = \frac{mc_p}{A_c U_L}\left[1 - \exp\left(-\frac{A_c U_L F'}{mc_p}\right)\right]. \tag{31}$$

and the heat collection rate (useful heat gain) in terms of the heat removal factor is

$$q_u{}'' = A_c F_R\left[I_T(\tau\alpha) - U_L(T_i - T_a)\right]. \tag{32}$$

The above set of Eqs. (1) to (27) constitutes a nonlinear mathematical model for the calculation of net useful heat collection rate q_u and thermal efficiency η of the solar water heater. Equations (28) – (32) have been used for cross-check of the results.

III. Thermohydraulic Performance

For laminar flow in a smooth tube, the hydraulic development length is given by [23]

$$\frac{L_{hy}}{D_i} \approx 0.05\,\mathrm{Re}. \tag{33}$$

For small diameter tubes of solar water heater (internal diameter of the order of 11-14 mm), and the maximum flow Reynolds number of the order of 750, the hydraulically development length is small (of the order of 37.5 diameters at the maximum flow rate; even lower for the lower flow rates) compared to the usual length of the collector tube (of the order of 140-180 diameters) hence the effect of development length on the friction factor may be neglected and the following friction factor relation for fully developed flow may be used.

$$f = \frac{16}{\mathrm{Re}}. \tag{34}$$

The pressure loss from the known values of friction factor *f* and pumping power are calculated from:

$$\delta p = \frac{4 f L G_m^{\,2}}{2\rho_f D_i} \tag{35}$$

$$P = \left(\frac{m}{\rho_f}\right)\delta p. \tag{36}$$

Cortes and Piacentini [24] used effective thermal efficiency η_e for the thermohydraulic performance evaluation of solar collector, which is based on the net thermal energy output of a collector considering the pumping power required to overcome the friction to the flow of fluid. Since the operating cost of a collector depends on the pumping power spent, the effective efficiency based on the net energy gain is a logical criterion for the performance evaluation of the solar collector. The effective efficiency equation due to Cortes and Piacentini is

$$\eta_e = \frac{\left(q_u - P/C\right)}{I_T A_c}, \tag{37}$$

where *C* is a conversion factor to calculate the equivalent thermal energy for obtaining the pumping power. It is a product of the efficiencies of the pump, electric motor, power transmission and thermoelectric conversion. Based on assumption of about 70% efficiency of the pump-motor combination and about 30% efficiency of thermoelectric conversion process referred to the consumer point, the factor *C* has been taken as 0.2 in the present study.

It is to mention that the model presented here for once-through smooth tube solar water heater can also be used for performance prediction of the water heater with enhanced tubes (tubes provided with heat transfer enhancement devices such as ribs, wire coil insert, twisted tape, spirally grooved tube with twisted tape insert, etc.) by using the heat transfer coefficient and friction factor relations for the enhancement device employed.

IV. Performance Prediction

The mathematical model has been solved for a given set of system and operating parameters following an iterative process. A computer program has been developed for this purpose. The flow chart of the program is given in Fig. 4. The steps involved in the solution are:

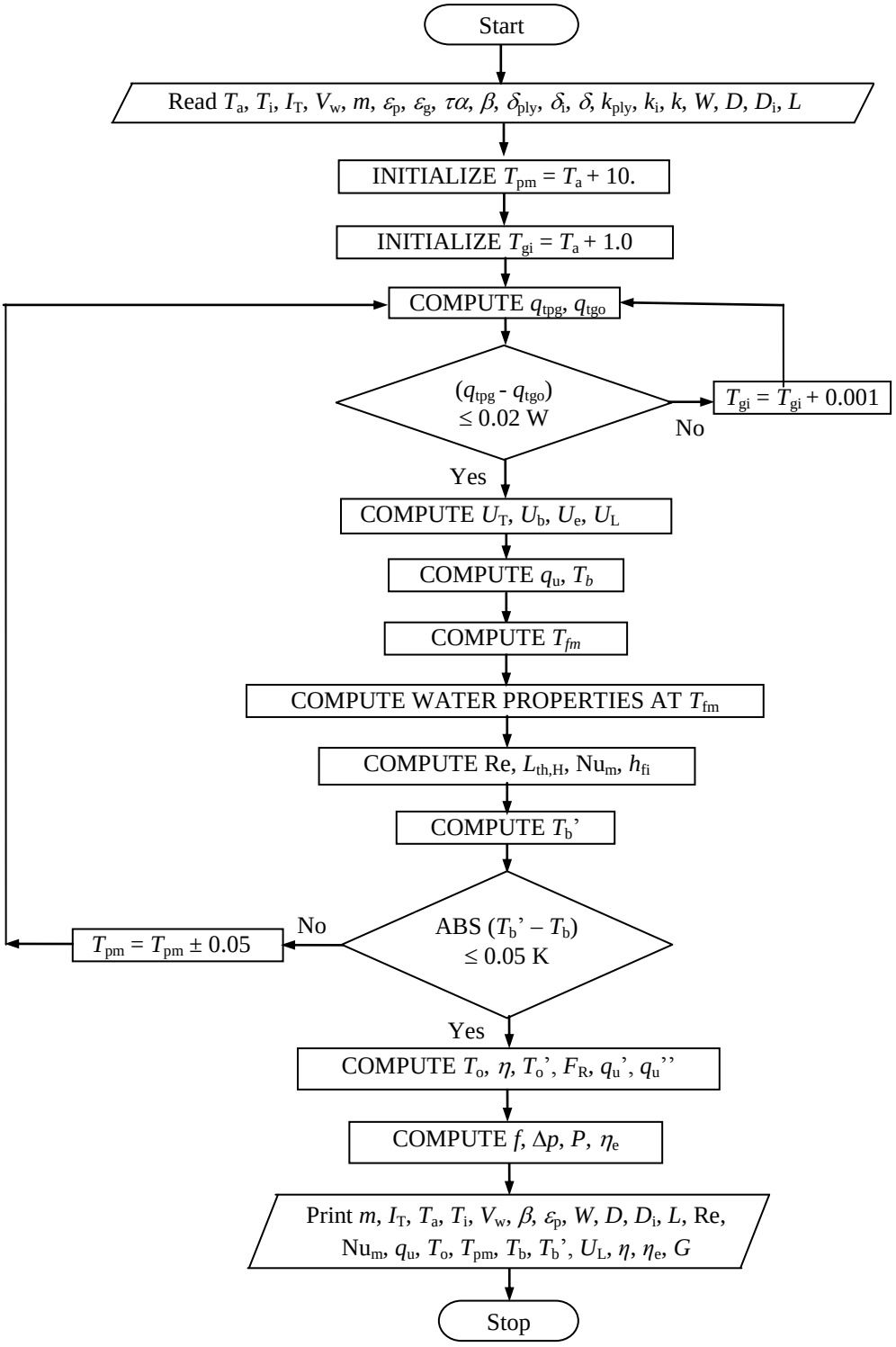

Fig. 4 Flow chart depicting the iterative solution method for the mathematical model.

Step 1: Initial estimate of the mean absorber temperature T_{pm} is made as mentioned in the flow chart.
Step 2: Initial estimate of the mean glass inner surface temperature T_{gi} is made as mentioned in the flow chart.
Step 3: Starting from the initial values of the mean absorber temperature and glass inner surface temperature, T_{gi} was increased in steps of 0.001 K till the heat loss estimate from the absorber surface to the glass cover q_{tpg} was not greater than 0.02 W from the estimate of heat loss from the glass cover to the ambient q_{tgo}.
Step 4: The top, back and edge loss coefficients, and the overall loss coefficient U_L are computed using Eqs. (9) – (12).

Step 5: The values of T_{pm} and U_L are used to calculate the useful heat gain q_u, and fin base temperature T_b from Eqs. (13) and (14), respectively.

Step 6: Using the calculated value of q_u, the mean water temperature T_{fm} is calculated using Eq. (17). The thermophysical properties of the water are computed at mean water temperature.

Step 7: The Reynolds number Re of the flow through the tube and thermal development length L_{th} are calculated using Eqs. (19) and (20), respectively. The estimates of the Nusselt number Nu_m and heat transfer coefficient h_{fi} are made using Eqs. (21) and (22), respectively.

Step 8: Using heat transfer coefficient h_{fi} and q_u, the fin base temperature T_b' is calculated using Eq. (23).

Step 9: The fin base temperatures T_b and T_b' are compared. If these two temperatures differ by more than 0.05 K, the mean absorber temperature is changed to $T_{pm} \pm 0.05$ K depending on whether $T_b' > T_b$ or $T_b' < T_b$. The steps 2 to 8 are repeated till ABS($T_b' - T_b$) ≤ 0.05 K.

Step 10: Water outlet temperature T_o, from known values of q_u and mass flow rate of the fluid, and the thermal efficiency η are calculated using Eqs. (26) and (27), respectively.

Step 11: For the cross-check of the results, water outlet temperature is also calculated as T_o' using Eq. (30), and q_u values q_u' and q_u'' are calculated using Eqs. (29) and (32), respectively. The value T_o' has been found to be within 0.1 K of value of T_o from Steps 1-10, while the difference in q_u values (q_u, q_u' and q_u'') has been found to be less than 0.5 W.

Step 12: Compute friction factor f, pressure drop Δp, pumping power P and effective efficiency η_e using Eqs. (34) - (37).

V. Validation of Mathematical Model

Values of the collector parameters used for the prediction of the thermal performance are listed in Table 1, where the geometrical parameters refer to the experimental setup of Sharma and Karwa [15]. The operating parameters for prediction refer to the mean values of these parameters at experimental conditions of Sharma and Karwa. The bond conductance has been calculated for the bronze joint ($k_b = 26$ $Wm^{-1}K^1$) of average thickness and width of 5 mm.

The experimental and predicted values of thermal efficiency as function of the mass flow rate of water through the collector with smooth tube are presented in Fig. 5, where the experimental data are from Sharma and Karwa [15]. The average experimental and the predicted thermal efficiency values differ by about 4% (2.2 percentage points) with similar trends. The difference can mainly be attributed to the uncertainties in the estimates of wind heat transfer coefficient, sky temperature and the transmittance-absorptance product for the absorber-glass cover combination for the performance prediction.

For the estimate of the wind heat transfer coefficient, in addition to the correlation of McAdams used here, various correlations have been presented by the researchers [27-31]. For the wind velocity of 0-1 ms^{-1} of experimental condition, the predicted values from these correlations differ by 5 $Wm^{-2}K^{-1}$ [32].

In the present model, the sky temperature has been estimated from the Swinbank's relation for clear sky conditions. Another approximate empirical relation is also available [33] which is:

$$T_s = T_a - 6. \qquad (38)$$

A comparison of the predicted value of the sky temperature from these correlations for the ambient temperature at experimental conditions shows that Eq. (38) predicts a value higher by about 5 K at experimental condition. Further it is a common knowledge that the sky temperature depends on the sky condition [34], which varies because of the variation in atmospheric humidity, pollution, etc.

From the above discussion, it can be inferred that the estimates of the wind heat transfer coefficient and sky temperature have an uncertainty of 5 $Wm^{-2}K^{-1}$ and 5 K, respectively. The analysis using the mathematical model shows that, at the experimental conditions, a change of 5 $Wm^{-2}K^{-1}$ in the wind heat transfer coefficient estimate changes the thermal efficiency by 1.8% at the lowest flow rate of the study; an increase in the wind heat transfer coefficient increases the convection heat loss from the glass cover and vice versa. An increase of 5 K in the estimate of the sky temperature increases the predicted thermal efficiency by 1.5% at the lowest flow rate; an increase in the sky temperature increases the thermal efficiency because of lower radiation heat loss to the sky. Further it has been found that a change of 1% in the transmittance-absorptance product for the absorber-glass cover combination changes the thermal efficiency by about 1%. These effects are found to be lower at the highest flow rate of the experimental study.

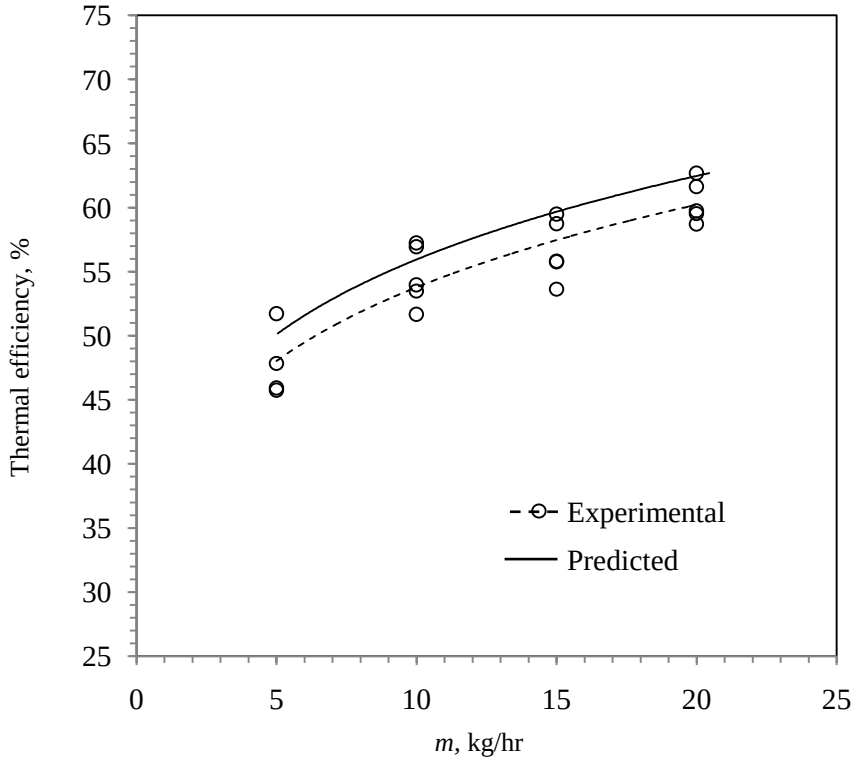

Fig. 5 Efficiency predicted versus experimental data of [15].

Table 1 Values of the collector parameters used for the validation of the thermal performance [15, 25, 26]

S. No.	Parameter	Values
1	Back plywood thickness, δ_{ply}	40 mm
2	Plywood thermal conductivity, k_{ply}	0.13 $Wm^{-1}K^{-1}$
3	Back insulation thickness δ_i (foamed polystyrene)	10 mm
4	Insulation thermal conductivity, k_i	0.037 $Wm^{-1}K^{-1}$
5	Gap between absorber plate and glass cover, δ_{pg}	40 mm
6	Long wave emissivity of glass, ε_g	0.88
7	Long wave emissivity of absorber surface, ε_p	0.9
8	Transmittance-absorptance product for absorber-glass cover combination, $(\tau\alpha)_{av}$	0.735*
9	Tube outside diameter, D	0.0235 m
10	Tube inside diameter, D_i	0.0195 m
11	Thermal conductivity of bond material, k_b	26 $Wm^{-1}K^{-1}$
12	Collector tilt, β	26^o
13	Fin width, W	0.1755 m
14	Fin thickness, δ_i	2 mm
15	Thermal conductivity of tube and fin material, k	386 $Wm^{-1}K^{-1}$

*$(\tau\alpha)_{av} = 0.96(\tau\alpha)_{beam} \approx 0.96\tau\alpha = 0.96 \times 0.85 \times 0.9 \approx 0.735$

Looking to the uncertainties in the estimates of wind heat transfer coefficient, sky temperature and transmittance-absorptance product for the absorber-glass cover combination, the matching of the predicted and experimental thermal efficiencies in Fig. 5 can be termed as excellent and the mathematical model can be used with confidence for the performance study of the once-through solar water heater.

VI. Parametric effect on Performance of the Solar Water Heater

6.1 Range and Values of Various Parameters

The range and values of various parameters for the present study are given in Table 2. The basic value of the collector slope β is 26^o (= the local latitude for year round operation), which has been varied by $\pm 15^o$ corresponding to the winter and summer conditions. Base value of the tube diameter (D/D_i = 12/10.8 mm) has been selected as per the present industrial practice. Larger diameter tubes give a smaller pressure drop penalty

and may affect the thermal performance hence the effect of increase in diameter has been studied. The width of the fin W per tube has been kept at 150 mm. The usual collector length L is 1.5-2 m because of the constraints of available size of plywood and glass sheets, and the ease of installation and handling. Inlet water temperature has been assumed to be the ambient temperature for once-through operation, which has been considered to vary from 278 K (lowest of the winter at Jodhpur) to 313 K (maximum of the summer at Jodhpur). The base value is taken as 293 K. The wind velocity has been considered from no wind to the usually encountered average value of about 2.0 ms^{-1} at Jodhpur.

The water mass flow rate per unit area of the absorber surface G is selected to give a temperature rise ΔT from about 5°-50°C. Solar insolation varies from lowest in morning and evening to maximum at the noon, which has been considered from 500 to 1000 Wm^{-2}.

It is to note that the major heat loss from the heated absorber is through the glass cover. The heat is transferred from heated absorber to the glass cover by convection and radiation. The radiation from the absorber is heat radiation. This heat loss is a strong function of the emissivity of the radiating surface. Ordinary blackboard painted absorber surface ($\varepsilon_p \approx 0.9$) has equal values of absorptivity for solar radiation and emissivity for heat radiation. Selective coatings have been suggested, which have excellent absorptivity for solar radiation but a low value of emissivity for the heat radiation ($\varepsilon_p \approx 0.1$). Hence, the effect of change of the emissivity of the absorber surface on the thermal performance of the collector has been investigated.

6.2 Thermal performance

The thermal performance results have been presented as plots of thermal efficiency versus the temperature rise parameter $\Delta T/I_T$ in Fig. 6 for the absorber surface emissivity of 0.1 and 0.9, and water mass flow rate G = 0.002-0.02 kgs^{-1} per m^2 of the absorber. These plots refer to fixed values of L = 2 m, W = 0.15 m, D = 12 mm, D_i = 10.8 mm, β = 26°, I_T = 800 Wm^{-2}, V_w = 1.0 ms^{-1}, $T_i = T_a$ = 293 K. The Reynolds number for these plots ranges from 110-750.

It can be seen from the plots in Fig. 6 that the thermal efficiency of collector with selective coating (ε_p = 0.1) on the absorber surface is significantly higher than that of the collector with absorber having blackboard paint (ε_p = 0.9). The advantage is comparatively higher at low flow rates when absorber temperature is high. Typically, at G = 0.002 $kgs^{-1}m^{-2}$, the thermal efficiency of the collector with selective coating is 53.16% as compared to 45.69% for the collector with blackboard paint. The corresponding values at G = 0.02 $kgs^{-1}m^{-2}$ are 66.51% and 61.00%, respectively. This improvement is because of the reduced radiation heat loss from the absorber. It must be noted that the selective coatings are costly as compared to the blackboard paint.

From the performance plots, it can be seen that at the lowest water flow rate G = 0.002 kg s^{-1} per m^2 of the absorber surface, the temperature rise parameter $\Delta T/I_T$ = 0.055 and 0.064 for collector with absorber surface emissivity of 0.9 and 0.1, respectively, which gives a water temperature rise ΔT of 55°C and 64°C for maximum solar insolation of around 1000 Wm^{-2} at Jodhpur. At the highest water flow rate of the study (G = 0.02 kgs^{-1} m^{-2}), the same works out to be 8°C for the collector with emissivity of 0.1.

It is to note that, at all flow rates under the study, the thermal and effective efficiency values have been found to differ marginally only. This behaviour is because of the very small pumping power requirement of the collector designs under study; the pressure loss is only 33.91 Nm^{-2} even at the highest flow rate of the study.

The use of performance plots of Fig. 6 is being illustrated here by taking an example. Let the temperature rise requirement is 25°C when solar insolation I_T is 800 Wm^{-2}. The temperature rise parameter ($\Delta T/I_T$) works out to be 0.03125. A vertical line on the graph from $\Delta T/I_T \approx 0.031$ cuts the plot for ε = 0.1 at $G \approx$ 0.045 $kgs^{-1}m^{-2}$ with a thermal efficiency of about 60 %.

The plots in Fig. 6 refer to fixed values of geometrical and ambient parameters as mentioned in the caption of the figure. However, the ambient parameters are variable and the design parameters may vary for different designs. Hence, the effect of variations in the design and ambient parameters on the collector thermal performance has been studied

6.3 Effect of Variation in Design and Ambient Parameters

In order to investigate the effect of variation of design and ambient parameters, one parameter has been varied at a time from the basic values of these parameters in Fig. 6. Most of the results are given in tabulated form, which may be useful for a designer.

Table 2 Range and values of various parameters for performance study.

Parameter	Range
Transmittance-absorptance product, $\tau\alpha$	0.735 (fixed) for single glass cover
Gap between the absorber plate and glass cover, δ_{pg}	40 mm [19]

Collector slope or tilt, β	$26^o \pm 15^o$
Back and edge insulation	Foamed polystyrene or glass wool
Thermal conductivity of insulation, k_i	0.037 $Wm^{-1}K^{-1}$
Back insulation thickness, δ_i	20-60 mm
Long wave emissivity: Glass cover, ε_g	0.88
Absorber surface, ε_p	0.9 (black-paint), 0.1 (selective coating)
Length of the collector duct, L	1.5 and 2 m
Tube diameter, D/D_i	12/10.8 mm, 15/13.6 mm
Width of absorber surface per tube, W	0.15 mm (fixed)
Fin thickness, δ	0.5, 1 and 2 mm
Thermal conductivity of bond material, k_b	26 $Wm^{-1}K^{-1}$ for brazed
	386 $Wm^{-1}K^{-1}$ (copper) for ultrasonic weld
Solar insolation, I_T	500-1000 Wm^{-2}
Wind velocity, V_w	0 (no wind),
	2 ms^{-1}
Mass flow rate per unit area of absorber, G	0.002- 0.02 $kgs^{-1}m^{-2}$
Sky temperature, T_s	= 0.0552 $T_a^{1.5}$ [18],
	= 0.0552 $T_a^{1.5}$ + 10 [34]
Ambient Temperature, T_a	278-313 K
Flow Reynolds number, Re	About 80–750

6.3.1 Tube diameter D_i

From the results given in Table 3(a), it can be seen that the change in the tube diameter (D/D_i) from 12/10.8 mm to 15/13.6 mm has insignificant effect on the collector thermal efficiency. The Nusselt number for the laminar flow in a tube is independent of the flow Reynolds number. The heat transfer coefficient for the larger diameter tube is lower than for the smaller diameter tube, but the product ($h_{fi}A = h_{fi}\pi D_i L$) has been found to be the same hence the thermal performance is not affected. The pressure drop for the larger diameter tube can be seen to reduce by 60% mainly because of the reduced mass velocity of water.

6.3.2 Fin thickness and bond conductance

Fin thickness has been varied from 0.5 to 2 mm. The thermal efficiency increases with increase in the fin thickness as seen in Table 3(b) because of the lower resistance offered by a thick fin to conduction heat flow to the tube (seen as increased efficiency F of the fin). It is to note that the thick fins can be brazed to the tube while the thin fins are to be joined with ultrasonic or laser beam welding. The brazing material of the joint has a lower thermal conductivity of 26 $Wm^{-1}K^{-1}$ [22] as compared to the ultrasonic or laser beam welded joint that has the same conductance as the fin and tube material. For copper tube and fin, thermal conductivity has been taken as 386 $Wm^{-1}K^{-1}$ [22]. It has been found that the ultrasonic or laser welded 0.5 mm fin shows practically the same performance as the 2 mm thick brazed fin. Though a thin fin offers greater resistance to heat flow by conduction, the welded thin fin offers the same performance as the brazed thick fin because of the low resistance of the welded joint as compared to the brazed joint of thick fin. There is a significant reduction in the weight of the fin and hence in the total mass of the tube and fin when a thin fin is used which compensates the increased cost of the ultrasonic or laser weld.

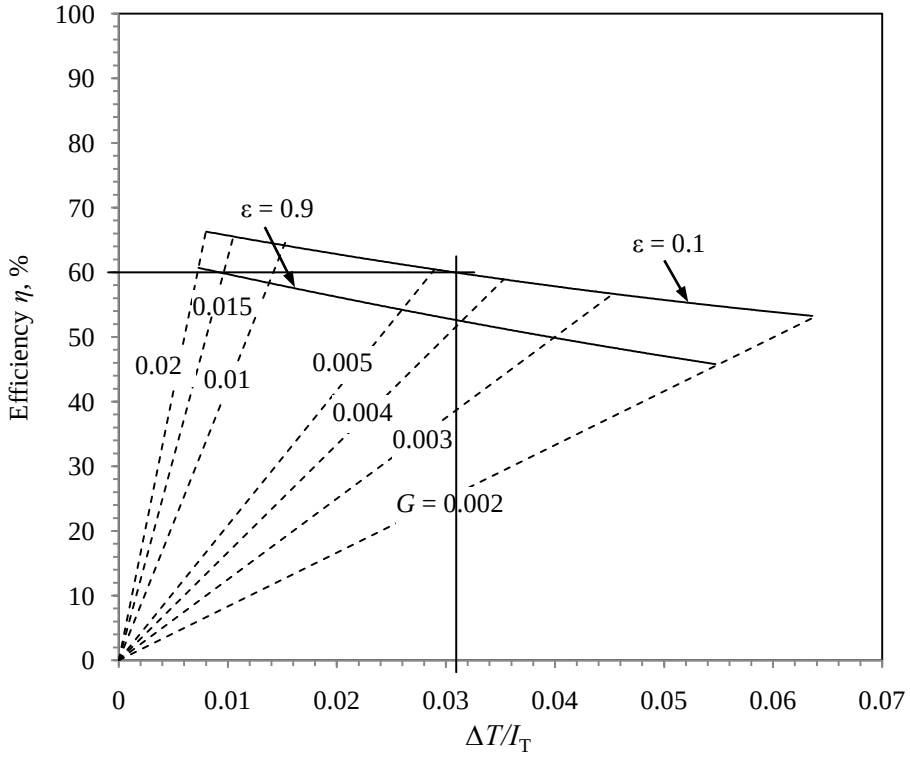

Fig. 6 Performance plots (L = 2 m, W = 0.15 m, D = 12 mm, D_i = 10.8 mm, β = 26°, I_T = 800 Wm^{-2}, V_w = 1.0 ms^{-1}, $T_i = T_a$ = 293 K).

6.3.3 Collector length *L*

From the results given in Table 3(c), it can be seen that a reduction in the collector length (i.e. the tube length) from 2 m to 1.5 m does not affect the thermal efficiency and the outlet temperature of the water because, for the fixed value of mass flow rate per unit area of the collector G, the mass flow rate per tube ($m = GWL$) reduces. Because of the reduced mass flow rate, the pressure drop is lower for collector with smaller length.

For a given collector area, the number of tubes (hence the collector width) is to be increased to accommodate the given total mass flow rate for the collector with smaller length. Such collector will require lower pumping power ($\delta p.nm/\rho$, where n is the number of tubes).

6.3.4. Collector tilt *β*

For winter operation, collector tilt higher by 10–20° than the latitude of the place is recommended, i.e., 36°-46° for Jodhpur (latitude = 26°). For summer operation, 10–20° lower tilt is recommended, i.e., 6°-16° for the place of study. For year round optimum performance, the collector tilt must equal the latitude of the place. The performance plots in Fig. 6 have been drawn for slope β = 26°. Thus this angle deviates from the optimum angles for summer and winter. The effect of variation of tilt by ±15° on the performance has been shown in Table 3(d) for solar insolation of 800 Wm^{-2}.

It can be seen that this variation has insignificant effect on the thermal efficiency; of the order of 0.3% maximum. Since the sensitivity of the collector performance is small to the variation of the tilt or slope, a liberal tolerance of ±5° in collector installation may be allowed. However, it is to note that a collector surface will receive lower solar radiation when the incident beam radiation makes an angle with the normal to the collector surface. Hence, the effect of change of tilt must be considered along with the effect of change of insolation.

Table 3(a) Effect of tube diameter (ε = 0.9).

G ($kgs^{-1}m^{-2}$)	D/D_i (mm)	η (%)	h_{fi} ($Wm^{-2}K^{-1}$)	$h_{fi}\pi D_i L$ (WK^{-1})	δp (Nm^{-2})	Mass (tube and fin) (kg)
0.002	12/10.8	45.69	258.24	8.762	2.3	5.33
	15/13.6	45.72	205.08	8.762	0.91	5.40
0.02	12/10.8	61.00	351.17	11.915	33.91	5.33
	15/13.6	61.05	278.87	11.915	13.49	5.40

Table 3(b) Effect of fin thickness and bond conductance (ε = 0.9).

G ($kgs^{-1}m^{-2}$)	δ (mm)	η (%) (F, %)		Mass (tube and fin) (kg)
		k_b = 26 ($Wm^{-1}K^{-1}$)	k_b = 386 ($Wm^{-1}K^{-1}$)	
0.002	0.5	44.51 (94.1)	**45.57** (94.1)	1.62
	1.0	45.29 (96.9)	46.39 (96.9)	2.86
	2.0	**45.69** (98.4)	46.80 (98.4)	5.33
0.02	0.5	59.06 (93.8)	**60.81** (93.7)	1.62
	1.0	60.34 (96.7)	62.43 (96.7)	2.86
	2.0	**61.00** (98.3)	63.40 (98.4)	5.33

Table 3(c) Effect of collector tube length (ε = 0.9).

G ($kgs^{-1}m^{-2}$)	L (m)	η (%)	T_o (K)	Re	f	Δp (Nm^{-2})	m (kgs^{-1})
0.002	2.0	45.69	336.72	111.5	0.1435	2.30	0.0006
	1.5	45.69	336.72	83.6	0.1913	1.29	0.0045
0.02	2.0	61.00	298.84	751.7	0.0213	33.91	0.006
	1.5	61.00	298.84	563.8	0.0284	19.08	0.0045

Table 3(d) Effect of tilt (ε = 0.9).

G ($kgs^{-1}m^{-2}$)	β (degree)	η (%)	U_L ($Wm^{-2}K^{-1}$)
0.002	26	45.69	7.20
	41	45.82	7.14
	11	45.61	7.23
0.02	26	61.00	7.80
	41	61.09	7.74
	11	60.96	7.83

Table 3(e) Effect of insulation thickness (ε = 0.9).

G ($kgs^{-1}m^{-2}$)	δ_i (mm)	η (%)	U_L ($Wm^{-2}K^{-1}$)
0.002	20	44.08	7.89
	40	45.69	7.20
	60	46.46	6.88
0.02	20	60.07	8.51
	40	61.00	7.80
	60	61.43	7.48

6.3.5 Insulation thickness δ_i

Increase in the back insulation thickness reduces the back loss. It has been found that an increase in the thickness from 40 mm to 60 mm improves the thermal efficiency by 0.7 to 1.7% depending on the flow rate; greater effect is seen at the lowest flow rate, refer Table 3(e). The decrease of the insulation thickness from 40 mm to 20 mm has greater effect on the thermal efficiency (1.55-3.65% decrease). It is to note the suggested insulation foamed polystyrene or glass wool is a low cost material and hence a liberal thickness of back insulation is recommended.

6.3.6. Solar Insolation I_T

Effect of variation of solar insolation from 500 to 1000 Wm^{-2} on thermal efficiency is found to be about 0.5-1%; higher effect is at the lowest flow rate. The effect is even lower for the collector with selective coating. It is to note that in the case of applications requiring constant outlet water temperature, the operation point will shift to the right in Fig. 6 when the insolation will decrease and the thermal efficiency will reduce significantly. For example, let the solar collector is operating at $\Delta T/I = 0.025$ when solar insolation is 800 Wm^{-2}. When the insolation decreases to 500 Wm^{-2}, the operating point will shift to $\Delta T/I = 0.04$ for a fixed value of ΔT and this will reduce the thermal efficiency to about 58% from 61.5% for the collector with selective coating.

A design is always based on an average value of solar insolation for a particular site hence percentage variation (±) in the performance with respect to the design value of solar insolation must be mentioned when the insolation varies during the day as well as with the month [35].

Table 4(a) Effect of wind velocity ($\varepsilon = 0.9$).

G ($kgs^{-1}m^{-2}$)	V_w (ms^{-1})	η (%)	U_L ($Wm^{-2}K^{-1}$)
0.002	0	46.71	6.78
	1.0	45.69	7.20
	2.0	45.00	7.49
0.02	0	61.13	7.71
	1.0	61.00	7.80
	2.0	60.91	7.86

Table 4(b) Effect of sky temperature ($\varepsilon = 0.9$).

G ($kgs^{-1}m^{-2}$)	T_s (K)	η (%)	U_L ($Wm^{-2}K^{-1}$)
0.002	T_s^*	45.69	7.20
	$T_s + 10$	46.92	6.70
0.02	T_s^*	61.00	7.80
	$T_s + 10$	62.60	6.63

*Calculated from Swinbank formula

6.3.7 Wind velocity V_w

The variation in the wind velocity from 0 to 2 ms^{-1} affects the thermal efficiency of the collector with $\varepsilon = 0.9$ by 3.8% at $G = 0.002$ $kgs^{-1}m^{-2}$ and 0.4% at $G = 0.02$ $kgs^{-1}m^{-2}$ as can be seen in Table 4(a). A high wind velocity causes greater top loss. The effect is more pronounced at lower flow rates because of the higher operating temperature of the absorber.

It has been found that a collector with selective coating on the absorber surface is comparatively less affected with variation in wind heat transfer coefficient; the thermal efficiency is affected by only 1.04% instead of 3.8% at $G = 0.002$ $kgs^{-1}m^{-2}$ and practically there is no effect at flow rate of 0.02 $kgs^{-1}m^{-2}$. Thus such collectors must be considered when the average wind velocity at the place of installation is high.

6.3.8 Ambient temperature T_a

It is an established fact that an increase in the ambient temperature reduces the thermal performance while a reduced ambient temperature improves the thermal performance [35]. The increase in the ambient and inlet temperature from 293 K to 313 K reduces the thermal efficiency of the collector with $\varepsilon = 0.9$ by about 0.73% at the lowest flow rate of the study while a decrease in the ambient temperature from 293K to 278K improves the thermal efficiency by 1.16%.

6.3.9 Sky temperature T_s

As mentioned earlier, the sky temperature is a function of many parameters and, in the case of large city areas, the sky temperature may be about 10°C higher than the one estimated from Swinbank's formula because of the atmospheric pollution [34]. The thermal efficiency improves with increase in the sky temperature due to the reduced heat loss by radiation from the surface of the glass cover. For a 10^oC increase in the sky temperature, the thermal efficiency has been found to increase by about 2.6-2.7% as can be seen in Table 4(b). The same effect has been found to be 1.77% maximum (at the lowest flow rate) when the absorber has selective coating.

VII. Effect of Heat Transfer Enhancement

Enhanced tubes (tubes provided with heat transfer enhancement devices such as fins, ribs, wire coil insert, twisted tapes, spirally grooved tube with twisted tape insert, etc.) can improve the thermal efficiency of the collector. More heat is transferred to the water with the enhancement in the heat transfer coefficient. This causes a reduction in the mean temperature of the absorber and hence the heat loss from the collector is reduced and thermal efficiency is increased.

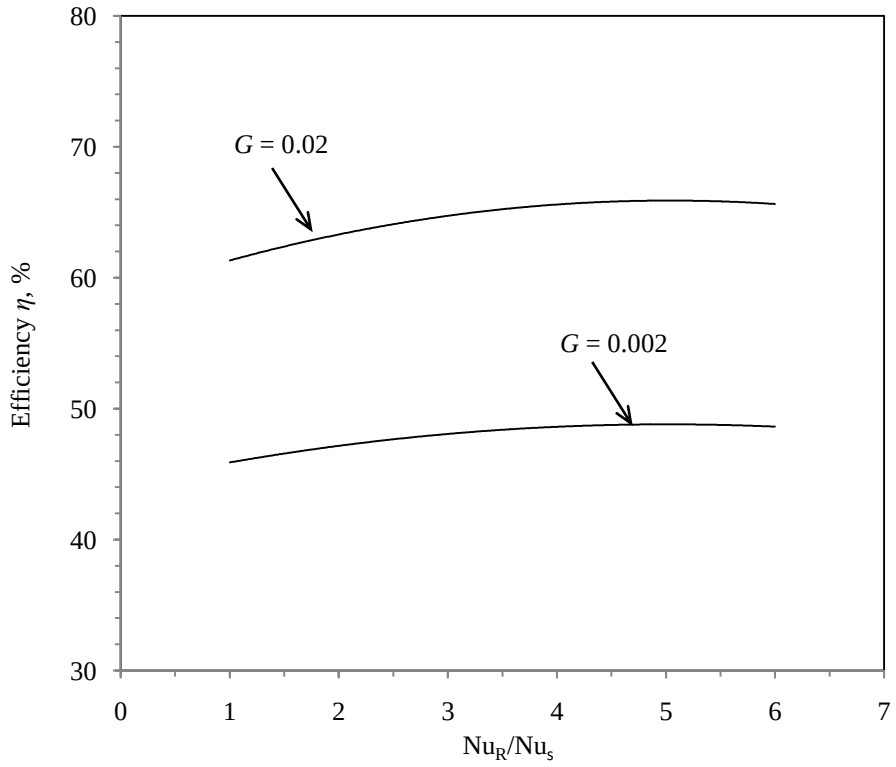

Fig. 7 Effect of heat transfer enhancement on thermal efficiency.

Figure 7 shows the effect of heat transfer enhancement (Nu_R/Nu_s) on the thermal efficiency at the lowest and the highest water flow rates of the study. The thermal efficiency increases with the increase in the enhanced tube Nusselt number as compared to the smooth tube; decreasing effect is seen with the increasing heat transfer enhancement. Typically $Nu_R/Nu_s = 3$ gives an enhancement of 5.3-6.2%; greater enhancement is at the highest flow rate. While for the enhancement in the heat transfer coefficient from $Nu_R/Nu_s = 3$ to 6, the additional advantage is 1.0-1.6% only. It must be noted that, in general as stated earlier, the pressure drop increases with the heat transfer coefficient enhancement hence it is prudent to go for devices providing heat transfer enhancement (Nu_R/Nu_s) up to 3. The enhancement in thermal efficiency of 5-6% can be termed significant because the additional cost of providing twisted tape is less than 2% of the total cost of the collector.

It has been mentioned earlier that the heat transfer enhancement due to use of twisted tape is also accompanied with significant increase in friction factor hence the choice of the enhancement device depends on the thermohydraulic consideration. Typically, Sharma [16] found that 75% width twisted tape with twist ratio of 2.5 enhances the Nusselt number by 130-150% ($Nu_R/Nu_s = 2.3$-2.5) and friction factor by 580-730% ($f_R/f_s = 6.8$-8.3). Thus the pressure loss for the twisted tape of Sharma [16] in 10.8 mm inner diameter tube comes out to be about 23-28 mm of water gauge for 2 m length of the tube. The pressure loss can be reduced significantly by using larger diameter tube as discussed earlier. The heat transfer enhancement at equal pumping power due to employment of the tape has been reported by Sharma to be 1.8-2 times. Thus from the thermo-hydraulic consideration also the twisted tape can be employed with advantage.

VIII. Conclusions

A mathematical model for thermohydraulic performance study of a once-through solar water heater has been presented, which has been validated against experimental data. The model has been utilized to study the collector performance for a range of design and ambient parameters, and flow rate (D/D_i = 12/10.8 and 15/13.6 mm, δ = 0.5-2.0 mm, δ_i = 20-60 mm, β = 26±15^o, L = 1.5 and 2 m, ε_p = 0.1 and 0.9, T_a = 273-313 K, V_w = 0-2.0 ms^{-1}, I_T = 500-1000 Wm^{-2}, and G = 0.002-0.02 kgs^{-1}m^{-2}). Both brazed and ultrasonic/laser welded designs have been considered. Effect of heat transfer enhancement on the thermal efficiency and pressure loss has also been studied.

The results of the study are presented in the form of plots for fixed values of L = 2 m, W = 0.15 m, D = 12 mm, D_i = 10.8 mm, β = 26^o, I_T = 800 Wm^{-2}, V_w = 1.0 ms^{-1}, $T_i = T_a$ = 293 K, δ = 2 mm (brazed), and ε_p = 0.1 and 0.9 along with the results and discussion of the effect on thermal efficiency and pressure drop due to variations over a range in design and ambient parameters, and flow rate.

The important findings of the study are:

1. At all flow rates of the study, the thermal and effective efficiency values differ marginally only for the smooth tube collector because of the very small pumping power requirement even at the highest flow rate of the study.
2. Collector with selective coating (ε = 0.1) has a thermal performance advantage of 9-16% depending on the flow rate.
3. A collector with 2 mm thick fins brazed or 0.5 mm thick fins laser or ultrasonic welded have practically the same performance.
4. Increase in the back insulation thickness from 20 mm to 60 mm is seen to increase the collector thermal efficiency by 2.3 to 5.4% depending on the flow rate.
5. At the lowest flow rate of the study, the wind velocity variation (0-2 ms^{-1}) affects the performance by 3.8%. The same is of the order of 1% for collector with selective coating.
6. Use of the heat transfer enhancement devices, such as twisted tape, can improve the thermal efficiency of the collector by 5.3-6.2% for three times heat transfer enhancement.

Nomenclature

A_c	Area of collector surface, m^2
A_e	Area of edge of the collector, m^2
c_p	Specific heat of water, Jkg^{-1} K^{-1}
D	Outer diameter of the tube, m
D_i	Inner diameter of tube, m
f	Fanning friction factor
F	Fin efficiency
F'	Collector efficiency factor
F_R	Heat removal factor
g	Acceleration due to gravity, ms^{-2}
G	Flow rate per unit area of absorber, kgs^{-1}m^{-2}
G_m	Mass velocity, kgs^{-1}m^{-2}
h	Heat transfer coefficient, Wm^{-2}K^{-1}
H	Twist pitch, m
h_{fi}	Heat transfer coefficient for tube flow, Wm^{-2}K^{-1}
h_w	Wind heat transfer coefficient, Wm^{-2}K^{-1}
I_T	Solar irradiance on collector plane, Wm^{-2}
k	Thermal conductivity of fin and tube material, Wm^{-1}K^{-1}
k_b	Thermal conductivity of bond material, Wm^{-1}K^{-1}
k_f	Thermal conductivity of water, Wm^{-1}K^{-1}
k_g	Thermal conductivity of glass, Wm^{-1}K^{-1}
k_i	Thermal conductivity of insulation material, Wm^{-1}K^{-1}
k_{ply}	Thermal conductivity of plywood, Wm^{-1}K^{-1}
L	Length of tube, m
L_{th}	Thermal development length, m
L_{hy}	Hydraulic development length, m
m	Mass flow rate, kgs^{-1}
Nu	Nusselt number
P	Pumping power, W
Pr	Prandtl number

q Heat transfer rate, W
q_t Top loss, W
q_u Rate of useful heat extraction from the collector, W
Ra Rayleigh number
Re Reynolds number
S Solar radiation absorbed by collector per unit area of absorber, Wm^{-2}
T_a Ambient temperature, °C, K
T_b Fin base temperature, °C, K
T_{fm} Mean water temperature, °C, K
T_{gi} Glass inner surface temperature, °C, K
T_{go} Glass outer surface temperature, °C, K
T_i Inlet water temperature, °C, K
T_o Outlet water temperature, °C, K
T_{pm} Mean absorber surface temperature, °C, K
T_s Sky temperature, K
U_b Back loss coefficient, $Wm^{-2}K^{-1}$
U_e Edge loss coefficient, $Wm^{-2}K^{-1}$
U_L Overall loss coefficient, $Wm^{-2}K^{-1}$
U_T Top loss coefficient, $Wm^{-2}K^{-1}$
V_w Wind velocity, ms^{-1}
w width of tape, m
W Width of fin per tube, m
y Twist ratio = H/w

Greek symbols

α Absorptance of the collector absorber surface for solar radiation
β Collector tilt, deg
δ Thickness of fin, m
δ_g Thickness of glass, m
δ_i Thickness of insulation, m
δ_{ply} Thickness of plywood, m
δ_{pg} Gap between absorber plate and glass cover, m
δp Pressure drop, Pa
ΔT Temperature rise of water, °C, K
ε Emissivity
η Collector thermal efficiency
μ_f Viscosity of water, Pa s
ν Kinematic viscosity, m^2s^{-1}
ρ_f Density of water, kgm^{-3}
σ Stefan Boltzmann constant, $Wm^{-2}K^{-4}$
τ Transmittance of the glass cover

Subscripts

av average
b back, base
f fluid
g glass
m mean
o outlet
p absorber surface
R tube with twisted tape
s smooth
t top

References

[1]. Wang YF, Li ZL, Sun XL. Once-through solar water heating system. Solar Energy 1982; 29(6), 541-547.
[2]. Duffie JA, Beckman WA. Solar engineering of thermal processes. 3rd ed. New Jersey: Wiley; 2006.
[3]. Wang L, Sunden B. Performance comparison of some tube inserts. Int Comm Heat and Mass Transfer 2002; 29, 45–56.
[4]. Dewan A, Mahanta P, Sumithra Raju K, Suresh Kumar P. Review of passive heat transfer augmentation techniques. Proceedings of the Institution of Mechanical Engineers, Part A: J. Power and Energy 2004; 218, 509-527.

[5]. Agarwal SK, Raja Rao M. Heat transfer augmentation for the flow of a viscous liquid in circular tubes using twisted tape inserts. Int J Heat and Mass Transfer 1996; 39(17), 3547-3557.
[6]. Kumar A, Prasad BN. Investigation of twisted tape inserted solar water heaters- heat transfer, friction factor and thermal performance results. Renewable Energy 2000; 19(3), 379-398.
[7]. Chang SW, Yang TL, Liou JS. Heat transfer and pressure drop in tube with broken twisted tape inserts. Experimental Thermal and Fluid Science 2007; 32(2), 489-501.
[8]. Bharadwaj P, Khondge AD, Date AW. Heat transfer and pressure drop in a spirally grooved tube with twisted tape insert. Int J Heat and Mass Transfer 2009; 52(7-8), 1938-1944.
[9]. Patil AG. Laminar flow heat transfer and pressure drop characteristics of power law fluids inside tubes with varying width twisted tape inserts. ASME J Heat Transfer 2000; 122, 143-149.
[10]. Abu-Khader MM. Further understanding of twisted tape effects as tube insert for heat transfer enhancement. Int J Heat and Mass Transfer 2006; 43, 123-134.
[11]. Jaisankar S, Radhakrishnan TK, Sheeba KN. Studies on heat transfer and friction factor characteristics of thermosyphon solar water heating system with helical twisted tapes. Energy 2009a; 34, 1054-64.
[12]. Jaisankar S, Radhakrishnan TK, Sheeba KN. Experimental studies on heat transfer and friction factor characteristics of thermosyphon solar water heater system fitted with spacer at trailing edge of twisted tapes. Applied Thermal Engineering 2009b; 29(5-6), 1224-1231.
[13]. Jaisankar S, Radhakrishnan TK, Sheeba KN, Suresh, S. Experimental investigation of heat transfer and friction factor characteristics of thermosyphon solar water heater system fitted with spacer at trailing edge of left-right twisted tapes. Energy Conversion and Management 2009c; 29(5-6), 2638-2649.
[14]. Sarma PK, Subrahmanyam T, Kishore PS, Rao VD, Kakac S. Laminar convective heat transfer with twisted tape inserts in a tube, Int J Thermal Sciences 2003; 42(9), 821-828.
[15]. Sharma Chandresh, Karwa Rajendra. Experimental study on an enhanced performance solar water heater. Int J Computer Applications (0975 – 8887) 2014**,** National Conf. on Advances in Technology and Applied Sciences, March 28-19, 2014, JIET School of Engineering & Technology for Girls, Jodhpur (India), 20-25.
[16]. Sharma Chandresh. Performance study of solar water heater with augmented heat transfer. Ph.D. Thesis. Faculty of Engineering & Technology, Jodhpur National University, Jodhpur (Rajasthan), India; 2016.
[17]. McAdams WH. Heat transmission. New York: McGraw-Hill; 1954.
[18]. Swinbank WC. Long-wave radiation from clear skies. Q J Roy Meteor Soc 1963; 89, 339.
[19]. Buchberg H, Catton I, Edwards DK. Natural convection in enclosed spaces- a review of application to solar energy collection. ASME J Heat Transfer 1976; 98(2), 182-188.
[20]. Klein SA. Calculation of flat-plate collector loss coefficients. Solar Energy 1975; 17, 79-80.
[21]. Ebadian MA, Dong ZF. Forced convection, internal flow in ducts. In: Rohsenow WM, Hartnett JP, Cho YI, editors. Handbook of Heat Transfer. New York: McGraw-Hill; 1998 [Chapter 5].
[22]. Holman JP. Heat transfer. 10th ed. New York: McGraw-Hill; 2010.
[23]. Kays WM, Crawford ME. Convective heat and mass transfer. New Delhi: Tata-McGraw-Hill Publishing Co. Ltd; 1980.
[24]. Cortes A, Piacentini R. Improvement of the efficiency of a bare solar collector by means of turbulence promoters. Applied Energy 1990; 36, 253-261.
[25]. Karwa Rajendra. Investigation of thermo-hydraulic performance of solar air heaters having artificially roughened absorber plate. Ph.D. Thesis, University of Roorkee, Roorkee, India; 1997.
[26]. www.EngineeringToolBox.com (accessed March 2, 2016).
[27]. Watmuff JH, Charters WWS, Proctor D. Solar and wind induced external coefficients - solar collectors. Cooperation Mediterraneenne pour l'Energie Solaire, Revue Internationale d'Heliotechnique 1977; 2nd Quarter, 56.
[28]. Kumar S, Sharma VB, Kandpal TC, Mullick SC. Wind induced heat losses from outer cover of solar collectors. Renewable Energy 1997; 10(4), 613-616.
[29]. Test FL, Lessmann RC, Johary A. Heat transfer during wind flow over rectangular bodies in the natural environment. ASME J Heat Transfer 1981; 103, 262-267.
[30]. Akhtar N, Mullick SC. Existing correlations for wind heat transfer coefficient and impact on the top heat loss factor of flat-plate collectors with a single glass cover. J Solar Energy Society of India 1998; 8(2), 105-112.
[31]. Kumar Suresh, Mullick SC. Convective heat transfer from the top outermost cover of a flat plate solar collector at low wind speeds. J Solar Energy Society of India 2007; 17(1, 2), 87-93.
[32]. Karwa Rajendra, Baghel Shweta. Effect of parametric uncertainties, variations and tolerances on thermo-hydraulic performance of flat plate solar air heater. J Solar Energy 2014; Article ID 194764, 18 pages (2014). http://dx.doi.org/10.1155/2014/194764
[33]. Garg HP, Prakash J. Solar energy: fundamental and applications. New Delhi: Tata-McGraw-Hill; 2000.
[34]. Nowak H. The sky temperature in net radiant heat loss calculations from low-sloped roofs. Infrared Physics 1989; 29(2-4), 231-232.
[35]. Karwa Rajendra, Chauhan Kalpana. Performance evaluation of solar air heaters having v-down discrete rib roughness on the absorber plate. Energy 2010; 35(1), 398-409.

Rajendra Karwa and Chandresh Sharma, "Performance Study of Once-Through Solar Water Heater." IOSR Journal of Mechanical and Civil Engineering (IOSR-JMCE), vol. 15, no. 2, 2018, pp. 46-65.